Arabian Journal for Science and Engineering (2020) 45:5143–5152
https://doi.org/10.1007/s13369-020-04368-y

RESEARCH ARTICLE-MECHANICAL ENGINEERING

Performance Improvement of a Single PEM Fuel Cell Using an Innovative Flow Field Design Methodology

H. Kahraman[1] · **A. Coban**[1]

Received: 8 October 2019 / Accepted: 20 January 2020 / Published online: 29 January 2020

Abstract
Flow fields of polymer electrolyte membrane fuel cells (PEMFCs) are used to feed reactant gases over the surface of catalyst layer homogeneously and remove byproduct, water. Optimization of the flow field design would improve homogeneity of the gas distribution and pressure drop values resulting in higher power density values. Flow field designs inspired from veins of tree leaves have been analyzed and tested. A mathematical model has been conducted for verifying the experimental results. A decrease in pressure drop and homogeneous distribution of gasses without flooding was observed with our novel designs. The dimensions of the flow channels were selected based upon tree leaves that obey Murray's law. Semi cylindrical obstacles were fabricated on the ground to direct the gas flow to the gas diffusion layer. The effect of these obstacles was observed at high current values. The cell performance and current density–temperature distribution analysis showed performance improvement up to 42.1% in comparison with the standard serpentine design. Homogeneity of current and temperature distributions was also improved with the proposed design. Additionally, water removal was improved with the current design.

Keywords PEMFC · Flow field design · Nature-inspired design · Current density distribution

1 Introduction

Fuel cells are a developing energy technology, which offers major advantages and wide range of applications for mobile and stationary systems [1] such as high energy efficiency, vibration free quiet operation, portable structure and almost zero emissions [2]. Among others, polymer electrolyte membrane fuel cell (PEMFC) is considered to be one of the most promising candidates for commercialization [3]. Various applications from mW scale to MW scale are considered to be used for any energy-demanding applications [2]. The advantages of the PEMFC in comparison with other fuel cell types are their high power density, zero pollution, light weight, low operation temperature, quick start-up capability and long lifetime [4–6]. However, further improvements are required to reduce their costs, enhance their durability and further optimize and improve their performance. The performance of PEMFCs strongly depends on factors such as mechanical design, operating conditions, transport phenomena in the cells, electrochemical reaction kinetics and manufacturing process [7].

Delivery of reactants and removal of products from a PEMFC are crucial for optimum performance and durability. Flow field design of the bipolar plates is the main actor for these processes. Power capacity value of a PEMFC can be affected by the flow field design excessively [8]. Homogeneous current and temperature distribution in parallel with effective water removal is a required behavior from a PEMFC which directs the flow field design [9].

Understanding and improving liquid water transport throughout the cell has critical importance in PEMFC performance, since flooding has been identified as one of the main current-limiting processes. The ionic conductivity will decrease, if the cell membrane is too dry. On the other hand, the presence of flooding in the porous catalyst layer or the gas diffusion layer (GDL) affects the performance of PEM fuel cell in negative manner, leading to a high concentration potential loss [10]. Local flooding, which might be caused by poor or non-homogeneous reactant distribution, is a crucial issue to be taken into account, since it usually leads to

✉ A. Coban
acoban@subu.edu.tr

H. Kahraman
huseyink@subu.edu.tr

[1] Mechanical Engineering Department, Faculty of Technology, Sakarya University of Applied Sciences, 54187 Sakarya, Turkey

non-uniform current density and localized hot spots in the membrane [11]. On the other hand, uniform distribution of gasses enables uniform current density distribution which also enables uniform temperature distribution and limited condensation of liquid water. Furthermore, lower mechanical stresses on the membrane electrode assembly (MEA) are observed with effective water management [10, 12–16] and homogeneous reactant distribution [17–20].

Reactant distribution for different purposes in nature gave inspiration for flow field design of PEM fuel cells. Arvay et al. [21] summarized the current state of nature-inspired flow field designs for PEMFC. These designs were usually named as "bionic" or "biomimetic," and their potential for homogeneous reactant distribution and limited flooding was emphasized.

Nature-inspired flow field design usually focused on optimum reactant distribution, pressure drop and fraction ratios between channel width and space between channels. The two novel designs of Wang et al. [22] showed improvements in reactant transportation and liquid water removal. Similarly, Ramos-Alvarado et al. [23] worked with nature-inspired flow field design with different fraction ratios with 16, 64 and 256 outlets. However, their best design (256 outlet channels) did not show better overall performance than the standard parallel design. Roshandel et al. [24] also studied biologically inspired designs based on the structure of a leaf and compared it against a serpentine design with a modeling study. Their model showed that the biologically inspired design outperformed traditional serpentine and parallel designs. Transport characteristics in the nature-inspired flow channel with obstacles were analyzed by Perng et al. [25]. The presence of regular or staggered rectangular obstacles across the protuberant catalyst layer surface and narrowing flow channels with ribs was the novel point of their study. They have observed a cell performance improvement of approximately 8% with their modified flow field design. Finally, baffles and blocked channels were also studied by flow field designers [26–30] to increase the PEMFC performance.

The aim of this study is combining the two novel design methodologies that provide uniform gas distribution and effective water removal. Better transport phenomenon with the cylindrical obstacles and more homogeneous reactant distribution along the bionic flow channels was the driving factor to obtain higher performance under various current values.

2 Materials and Methods

2.1 MEA Preparation

Custom-made Pt/C catalyst particles, synthesized with a modified sodium borohydride reduction method previously reported [31], were used to prepare MEAs. Catalyst slurries containing Nafion, Pt/C catalyst, water, isopropanol and propanediol were coated on Teflon sheets homogeneously with the screen printing method. A silk screen with 100 mesh was masked to the desired active area, 50 cm^2, during the screen printing method. These coatings were transferred onto Nafion HP using the decal transfer method to prepare the MEAs. The coatings were transferred on both sides of Nafion HP under approximately 20 Bar pressure and 130 °C temperature. The details of the MEA preparation method are explained in our previous studies [32].

2.2 Flow Field Design

The bipolar plates used in this experiment were roughly 3 mm thick and machined with 1 mm diameter carbide end mills. Prior to machining the channels, both surfaces of the graphite plates were cleaned with a large tool. This step enabled homogeneous compression over the MEA/GDL and avoided gas leakage. The aluminum end plates were used for compression, and 300-µm-thick gold-plated copper plates were used as current collectors.

Conventional and custom-made designs were machined for comparison. Patterns inspired from leaf veins (Fig. 1) prepared with or without semi cylindrical obstacles (Fig. 2) following the Murray's law of branching were compared with conventional parallel and serpentine designs. The effects of these design criteria were monitored step by step.

The advantages and disadvantages of conventional flow field patterns (pin type, parallel, serpentine and interdigitated) have been deeply reviewed in the literature [33]. The purpose of distributing goods from a sole entrance to a large area homogeneously is the common ground between PEM fuel cells and natural structures, such as leaf veins and blood vessels. Both leaf veins and blood vessels have a gradual structure to distribute nutrients to their target. The geometrical structure at the bifurcation region enables minimum energy loss during transportation of the nutrients. Usually the length and diameter of the leaf veins and blood vessels decrease in size after the bifurcation zone. The law of nature actually follows the principle of minimum of work, also known as Murray's law [34]. According to this law, the cube of the radius of the parent vessel (vein, channel or etc.) is equal to the sum of the cubes of the radii of the daughter vessels branching from it. This theory was used to determine the channel dimensions of various nature-inspired designs, such as microfluidic networks [35, 36] and tissue engineering [37]. The application of Murray's law on PEM fuel cell flow channel design was also proposed by other researchers [38]. In this study, flow channel widths were determined according to Murray's law (Fig. 3) following Eq. (2.1), where r_p is the radius of the parent channel and

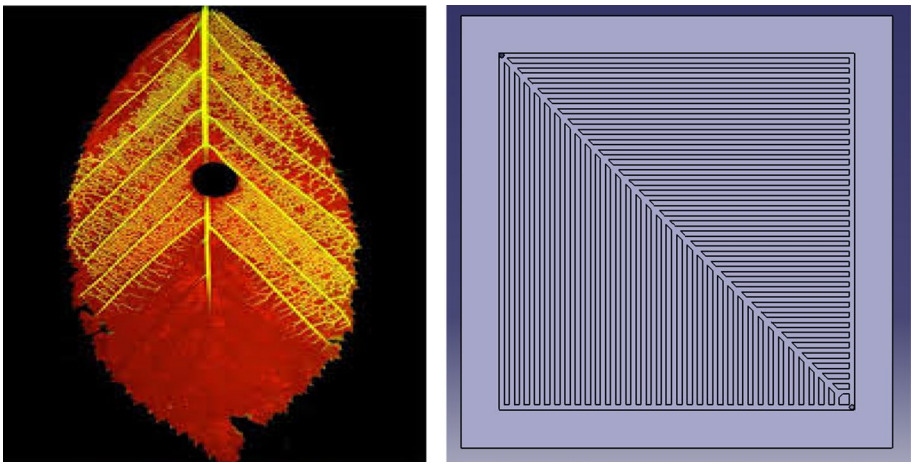

Fig. 1 Leaf veins and flow field channel application

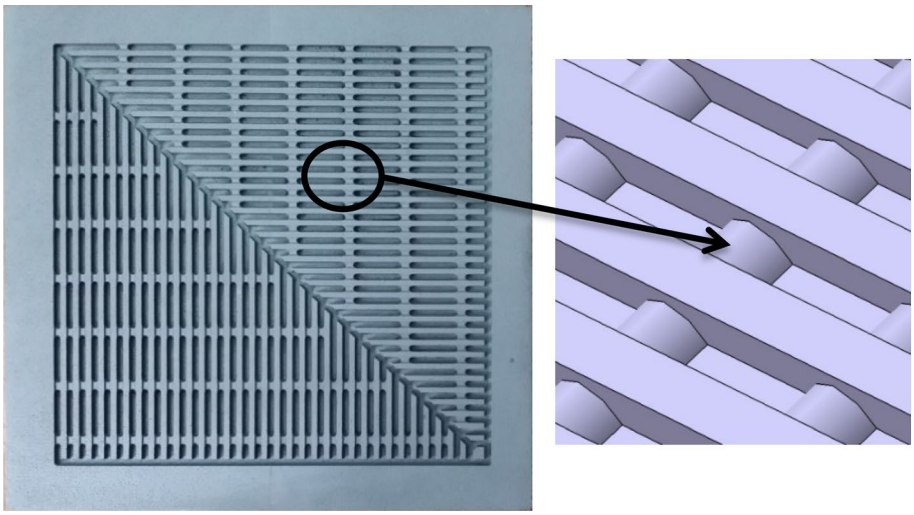

Fig. 2 Nature-inspired design with semicylindrical obstacles

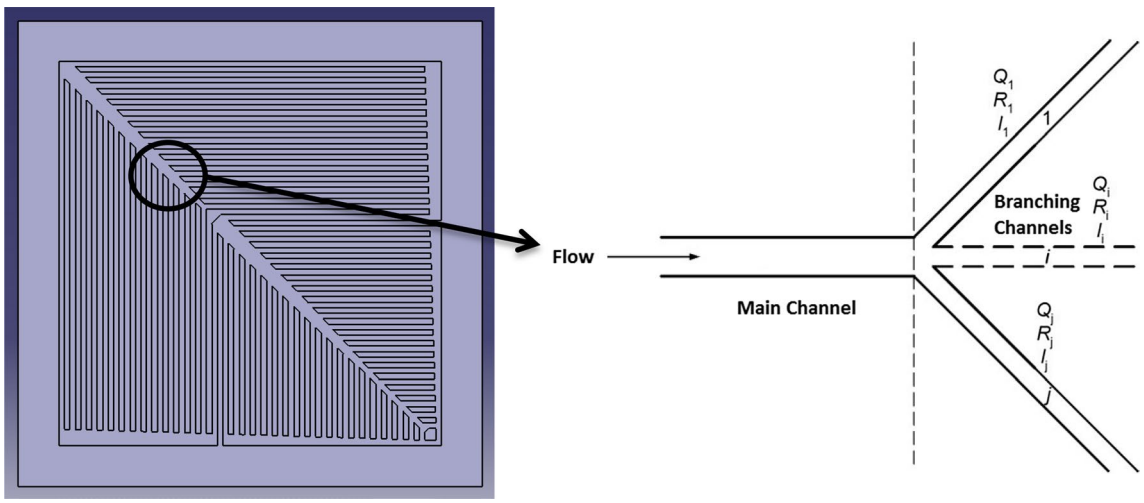

Fig. 3 Murray's law of branching and flow field channel application

r_{dn} ($n = 1, 2, 3, \ldots$) values are the radii of the branching channels:

$$r_{\mathrm{p}}^3 = r_{d1}^3 + r_{d2}^3 + \cdots + r_{dn}^3. \tag{2.1}$$

2.3 Mathematical Expressions

A model is only as accurate as its assumptions allow it to be. Assumptions used in fuel cell modeling are:

- Ideal gas properties
- Incompressible flow
- Laminar flow
- Isotropic and homogeneous electrolyte, electrode and bipolar material structures
- A negligible ohmic potential drop in components
- Mass and energy transport is modeling from a macroperspective using volume-averaged conservation equations.

Reactant flow in the fuel cell flow channels is very dependent upon the geometry of the channels. Regardless of the channel geometry, the governing equation is the conservation of mass in a fuel cell:

$$\frac{\partial \rho}{\partial t} + \nabla \cdot (\rho v) = \mathrm{S}_m \tag{2.2}$$

where ρ is the density, kg m^{-3}, v is the velocity vector, m s^{-1}, ∇ is the operator, $\frac{\mathrm{d}}{\mathrm{d}x} + \frac{\mathrm{d}}{\mathrm{d}y} + \frac{\mathrm{d}}{\mathrm{d}z}$, and S_{m} represents the additional mass sources.

Momentum conservation is described by Eq. (2.3):

$$\frac{\mathrm{d}(\rho v)}{\mathrm{d}t} + \nabla \cdot (\rho v) = -\nabla p + \nabla \cdot \left(\mu_{\mathrm{mix}} \nabla v\right) + S_{\mathrm{m}} \tag{2.3}$$

where p is the fluid pressure, Pa, μ_{mix} is the mixture average viscosity, kg m^{-1} s^{-1}, and S_{M} is the external body forces.

Material properties and reaction rates are a strong function of temperature. Therefore, it is important to account for temperature variations within the cell by solving the conservation of energy equation. Conversation of energy for any domain in a fuel cell is described by Eq. (2.4):

$$\left(\rho c_{\mathrm{p}}\right) \frac{\mathrm{d}T}{\mathrm{d}t} + \left(\rho c_{\mathrm{p}}\right)(v \cdot \nabla T) = \nabla \cdot \left(k_{eff} \nabla \mathrm{T}\right) + S_{\mathrm{e}} \tag{2.4}$$

where c_{p} is the mixture-averaged specific heat capacity (J kg^{-1} K^{-1}), T is the temperature (K), k is the thermal conductivity (W m^{-1} K^{-1}) and S_{e} is the energy source term. S_{e} includes the heat from reactions, ohmic heating and heat associated with a phase change.

The species balance equation represents mass conservation for each reactant. Species conservation for the gas phase is:

$$\frac{\partial(\varepsilon \rho x_i)}{\partial t} + \nabla \cdot \left(\varepsilon \rho x_i\right) = \left(\nabla \cdot \rho D_i^{\mathrm{eff}} \nabla x_i\right) + S_{s,i} \tag{2.5}$$

where x_{i} is the mass fraction of gas species, D^{eff} is a function of porosity and $S_{s,i}$ represents additional species sources.

In the Nafion membrane, two types of water flux are present: back diffusion and electroosmotic drag. Both fluxes can be accounted for by the following equation [39]:

$$J_{\mathrm{H_2O}}^{\mathrm{M}} = 2n_{\mathrm{drag}} \frac{i}{2F} \frac{\lambda}{22} - \frac{\rho_{\mathrm{dry}}}{M_{\mathrm{m}}} D_{\lambda} \frac{\mathrm{d}\lambda}{\mathrm{d}z} \tag{2.6}$$

The water content is not constant in Eq. (2.6). By obtaining the water content, the resistance of the electrolyte can be estimated.

2.4 Experimental Setup

In this study, a single PEM fuel cell with an active surface area of 50 cm^2 was used for all experiments. The MEA was made of Nafion® HP membrane and 45 wt% Pt/C catalyst layers with 0.2 and 0.4 mgPt/cm^2 loadings on the anode and cathode side, respectively. 200-micron-thick AvCarb EP40 GDLs were used in all experiments. The experiment setup was built with Bilvetek EY100 electronic load bank, two Aalborg DFC-26S-VAL5-C2 mass flow controllers, two Fuel Cell Technologies Nafion tube-type humidifiers, two heated gas lines, a multiple temperature controller (Bilvetek Inc.), two pressure regulators, two ball valves as humidifier bypass valves, H_2 and O_2 bottles and two backpressure regulators (Fig. 4). The fuel cell polarization curves were measured with the computer-controlled electronic load bank. The mass flow rates were set manually and read through the LCD display. The H_2 and O_2 flow rates were 0.168 L/min and 0.28 L/min that corresponded to a stoichiometry of 1.2 and 2 at 40 A (maximum) current, respectively. The cell temperature was set to 60 °C, and the humidifier temperatures (both anode and cathode) were set to 46 °C, 54 °C and 60 °C which corresponded to 50%, 75% and 100% relative humidity, respectively.

US Fuel Cell Council, Single Cell Test Protocol was used as a reference test protocol to obtain the polarization curves of the 50 cm^2 MEAs. The cell was kept at open-circuit potential (OCV) for 15 min; then, a constant current value of 10 A was applied for 30 min to ensure that the fuel cell reached a stable operating condition. Furthermore, the water removal capability of the flow field plate with different designs was observed by applying 10, 20, 30 and 40 A of current for 5 min each.

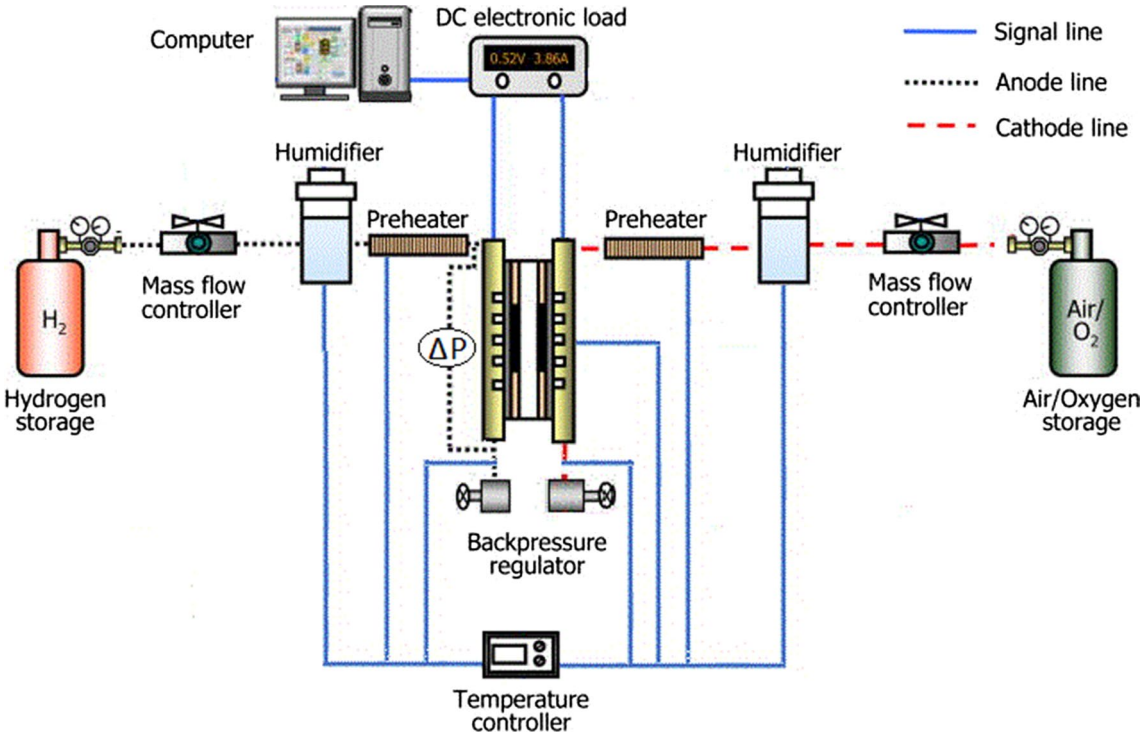

Fig. 4 Experimental setup

2.5 Current Density Distribution Measurements

PEM-type fuel cells work efficiently with precious catalysts prepared around 2–5 nm [40]. Each catalyst particle at this range can generate current if all reactants, gas, ion and electrons can reach the catalyst surface. Utilization of these precious catalyst particles is extremely important for cost/performance optimization. The flow field designs should be made considering maximum fuel utilization. Homogeneous gas distribution that can utilize all precious catalyst particles is required for homogeneous current production. Homogeneity of the current distribution is measured with a current scan board (S++ Simulation Services) that could measure current at $10 \times 10 = 100$ small segments for 50 cm^2 MEAs. The two-dimensional current and temperature map was obtained with this hardware at high resolution. The current scan board that was placed between the custom-made graphite flow field plate and gold-coated current collector plate could monitor two-dimensional (2D) current and temperature map at high resolution. The experimental apparatus is shown in Fig. 5.

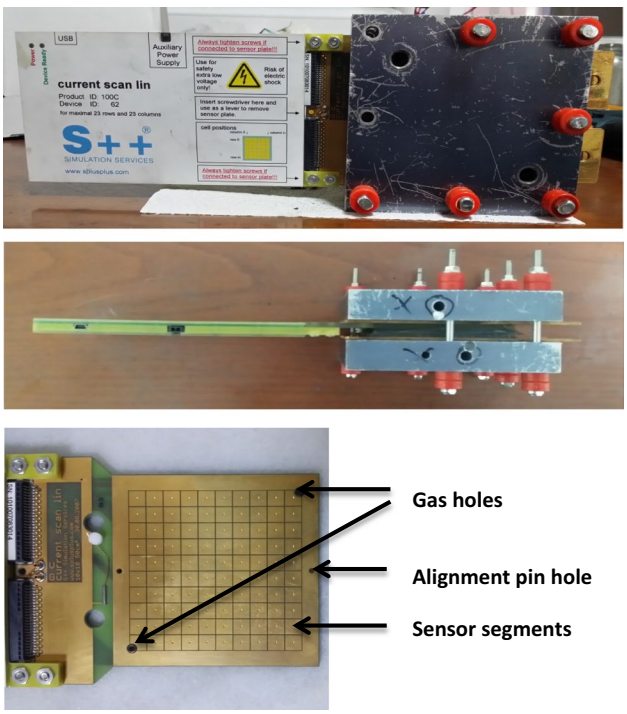

Fig. 5 50 cm^2 single cell and current scan board assembly

3 Results and Discussion

3.1 Performance Measurements

Four different channel designs, serpentine, the nature-inspired design (NID), the nature-inspired design with obstacles (NIDO) and the custom design that follows the Murray's law, have been tested at different current values and at a different relative humidity. Experiments conducted with pure H_2 and O_2 gasses at 60 °C cell temperature, 1.2 Nm compression torque, 1.5 Bar back pressure and 100% RH and constant flow rates equivalent to stoichiometry of 2 at maximum current are shown in Fig. 6. Additionally, a mathematical model has been added to the study for verifying the experimental results. The nature-inspired design (NID) and Murray design performed better than the conventional serpentine design (10–15% higher maximum power density). The channel width, channel depth and distance between the channels for the NID were all 1 mm. On the other hand, channel dimensions were changing for the design based on Murray's law. The minimum energy loss obtained with this design enabled faster penetration of the reactants on x- and y-axes (parallel to the flow field surface). However, the highest performance was observed with the NIDO. This performance improvement might be explained with the forced movement on z-axis (perpendicular to the flow field surface) with the help of semicylindrical obstacles. Forced movement on z-axis enabled reactants to penetrate through the adsorbed water films on the walls of the GDL and the catalyst layer. Furthermore, the velocity of the flow was also increasing when the gas flow was passing over the obstacles, since the section area was much lower at these regions. The velocity increase not only improved the penetration of the reactants, but also enabled dispersion of water droplets. An increase in Weber number was obtained with velocity increase, which indicates the ratio between the inertia force removing water from the reaction region and the surface tension adsorbing water on the walls. Even though the Weber number has negligible effect on drag coefficient of water flow [41], it has effect on breakup of water particles in multiphase flow [42]. The linear potential drop for the NIDO (Fig. 6) even at high current density values showed that water removal was very effective with this design, since no mass transport loss was observed. The experimental results of NIDO design are quite compatible with the theoretical results.

The two obstacle-free Murray and NID designs are compared in Fig. 7. The experiments were conducted at 40 °C cell temperature and constant flow rates of 0.168 L/min and 0.28 L/min for the anode and cathode, respectively, and a compression torque of 2.4 Nm. Several outcomes were obtained from the results. First of all, the cell resistance slightly decreased with increasing humidity for the Murray design. However, it was almost constant for the NID design. Both designs showed mass transfer losses at 100% RH value. This should be related to flooding due to insufficient water removal. The Murray design showed better performance against the NID design at high currents and at high humidity values. A performance improvement of 24.5% was obtained with the NID design against the Serpentine design at high current region (at 0.4 V) due to better water removal capability of this design. The Murray and NIDO designs performed even better than the NID design. The results are summarized in Table 1.

Constant current experiments were also conducted to observe continuity of the high performance obtained with these new designs. Experiments were conducted at 10 A, 20 A, 30 A and 40 A with the 50 cm^2 MEAs at 40 °C cell temperature and anode and cathode stoichiometry of 2 and 2.4 Nm compression torque. The results are compared in Fig. 8.

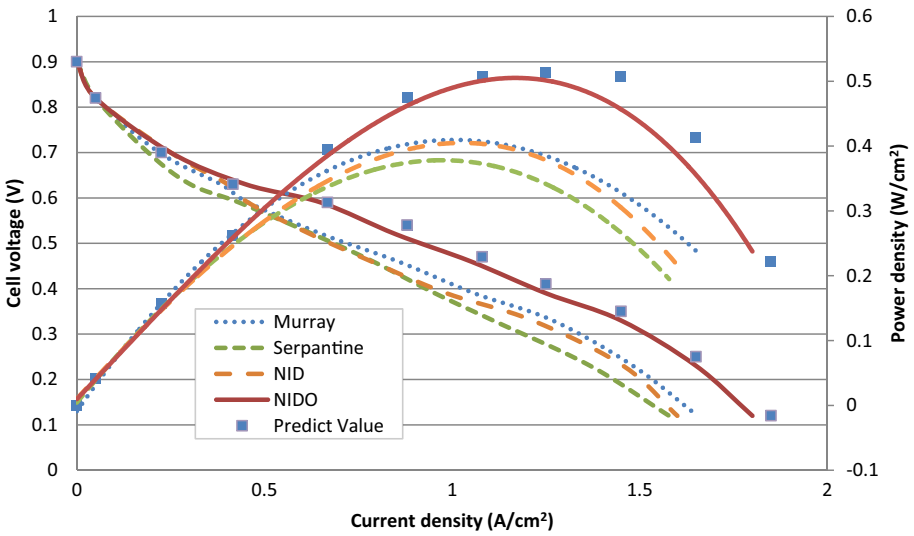

Fig. 6 Polarization and power density curves of all the samples

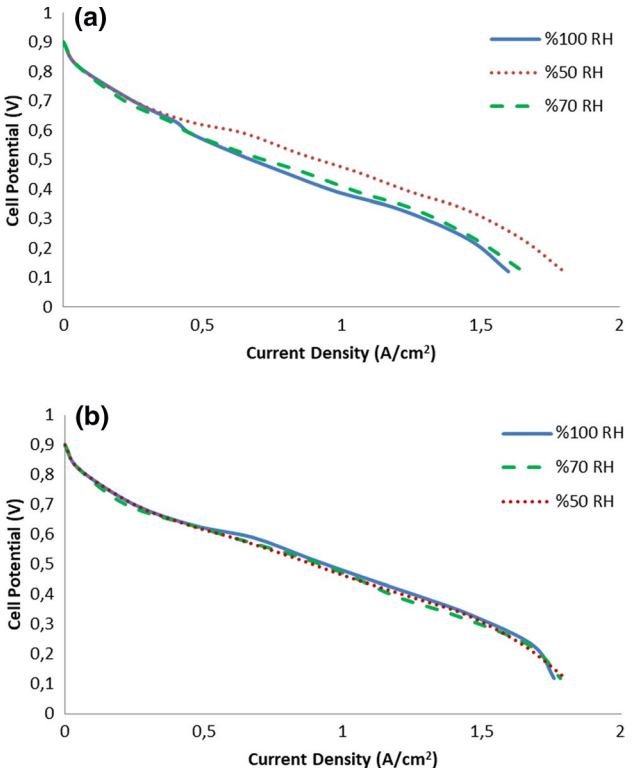

Fig. 7 Comparison of Murray design (**a**) with NID (**b**)

Table 1 Performance improvement summary

Design	Serpentine	NID	Murray	NIDO
Current density (A/cm^2) at 0.4 V	0.508	0.613	0.662	0.722
Performance improvement (vs. the serpentine design)	–	20.6%	30.3%	42.1%

The Murray and NIDO designs showed almost no performance drop at all current values; however, the serpentine and the NID designs showed serious performance drop at 40 A. These results proved that the water removal is improved with integrating obstacles in flow channels or by calculating the channel widths according to Murray's law of branching.

3.2 Current and Temperature Distribution Measurements

The current distribution in PEMFC is affected excessively from the flow channel design. The non-uniformity causes local temperature rises, flooding and fuel starvations. These extraordinary conditions can damage or decrease the utilization of the catalyst layer [43, 44]. Current density measurements were made to determine the poor performing spots

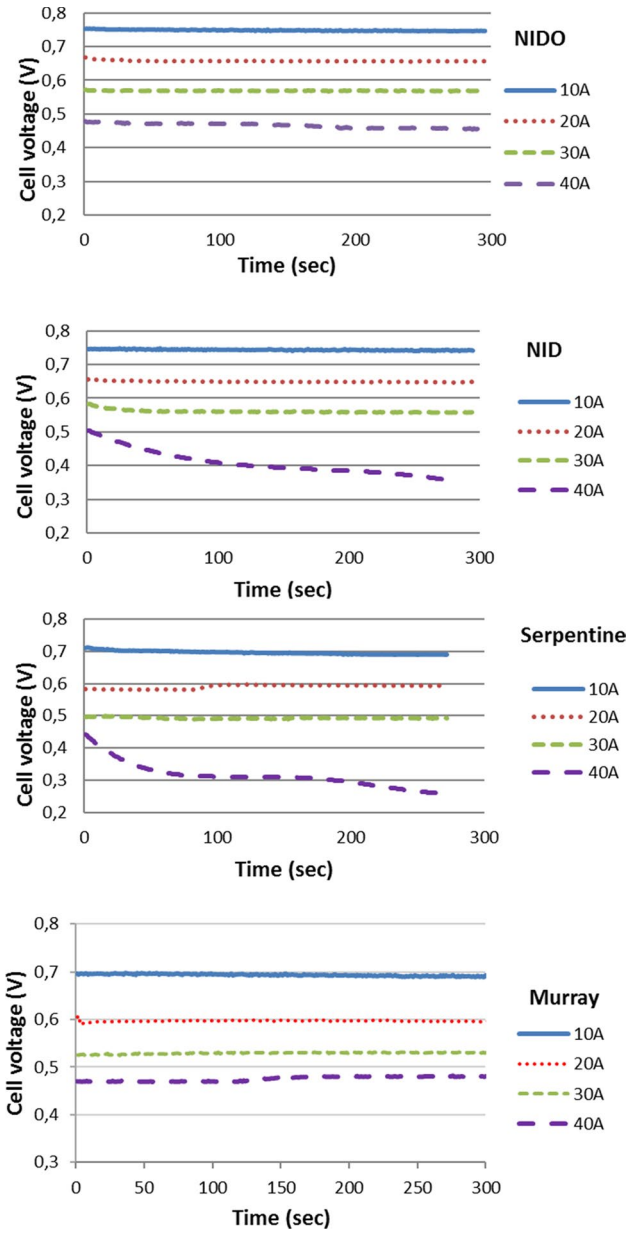

Fig. 8 Constant current measurement comparison of standard serpentine with Murray, NID and NIDO designs

and fluctuations in current for the serpentine, NID, Murray and NIDO designs. The input and outputs of the current distribution cell are shown in Fig. 9.

Figure 10 shows the current distributions for the serpentine design at low current and high current values. At low current case, the current distribution is homogeneous; however, huge oscillations were observed at high current case. The current values at the gas outlet ($y=0$) are smaller than the majority of the surface. The drop in stoichiometry and pressure, as well as the water formation, might be the reason for this local performance loss.

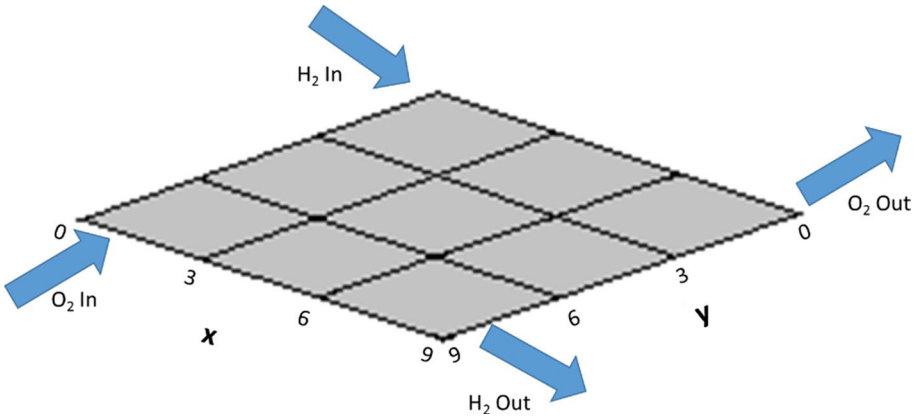

Fig. 9 Current distribution measurement cell structure

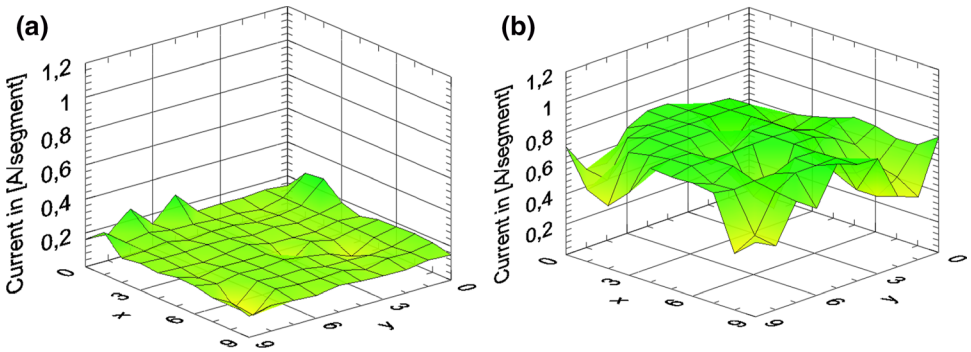

Fig. 10 Current distributions for serpentine design at 0.15 A/cm^2 (**a**) and at 0.5 A/cm^2 (**b**)

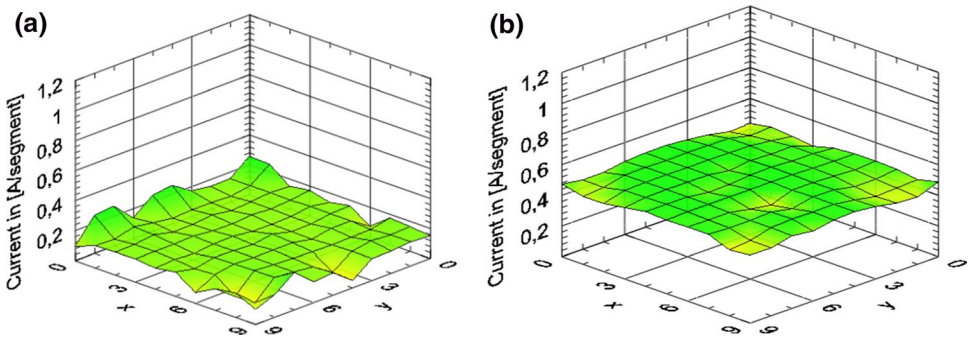

Fig. 11 Current distributions for NID design at different current density values

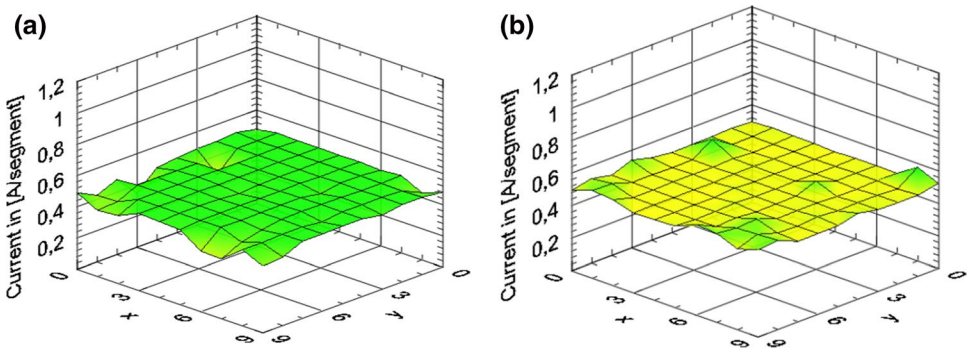

Fig. 12 Current distributions for **a** NIDO and **b** Murray designs

Current distribution for the NID design showed much more homogeneity against the serpentine design (Fig. 11). The drop in stoichiometry and pressure did not affect the current values as much as in serpentine design. The generated water molecules were removed from the flow channels more effectively in the NID design.

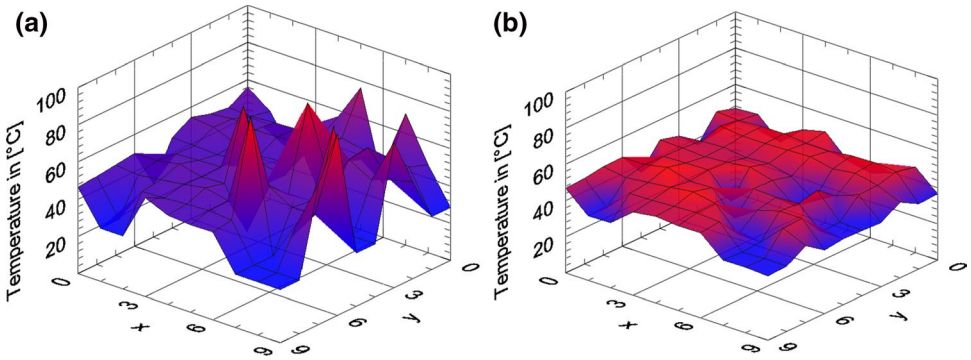

Fig. 13 Temperature distributions for **a** serpentine and **b** NID designs

The Murray and NIDO designs also showed homogeneous current distribution along the flow channels (Fig. 12). The fluctuation of current within the surface was very small.

The temperature distributions of the surfaces were in parallel with the current distributions. The temperature distribution of the serpentine and NID channels is shown in Fig. 13. The serpentine channel showed several local hot spots, whereas the NID design showed a very homogeneous temperature profile.

4 Conclusions

Nature-inspired flow channel design with (NIDO) and without obstacles (NID), the design following the Murray's law of branching (Murray) and typical serpentine design were manufactured and compared in terms of performance. Average current and current distributions were obtained for the bipolar plates prepared according to these designs. At high current region, the flow field type had enormous effect on performance. Among others, the highest performance improvement, 42.1% versus the serpentine design at 0.4 V, was obtained with the NIDO flow channels. On the other hand, the NID, Murray and NIDO had homogeneous current distribution, whereas the typical serpentine design showed inhomogeneity at certain regions at high current values. The positive effect of obstacles was observed in overall performance and continuity of the performance. In this study, the water management in PEM fuel cells was improved by combining two innovative approaches, the nature-inspired design and using obstacles. A mathematical model has been conducted for verifying the experimental results.

Acknowledgements The authors would like to thank Coordination of Scientific Research Projects of Sakarya University for their financial support (Project # BAP 2014-05-04-001) and Bilvetek Corp. for their technical support.

References

1. Kopanidis, A.; Theodorakakos, A.; Gavaises, M.; Bouris, D.: Pore scale 3D modelling of heat and mass transfer in the gas diffusion layer and cathode channel of a PEM fuel cell. Int. J. Therm. Sci. **50**, 456–467 (2011)
2. Sharaf, Omar Z.; Orhan, Mehmet F.: An overview of fuel cell technology: fundamentals and applications. Renew. Sustain. Energy Rev. **32**, 810–853 (2014)
3. Aiyejina, A.; Sastry, M.K.S.: PEMFC flow channel geometry optimization: a review. J. Fuel Cell Sci. Technol. **9**, 011011–1 (2012)
4. Chen, Shizhong; Xia, Zhongxian; Zhang, Xuyang; Yuhou, Wu: Numerical studies of effect of interdigitated flow field outlet channel width on PEM fuel cell performance. Energy Procedia **158**, 1678–1684 (2019)
5. Kuo, J.K.; Yen, T.S.; Chen, C.K.: Improvement of performance of gas flow channel in PEM fuel cells. Energy Convers. Manag. **49**, 2776–2787 (2008)
6. Wang, X.D.; Duan, Y.Y.; Yan, W.M.; Peng, X.F.: Effects of flow channel geometry on cell performance for PEM fuel cells with parallel and interdigitated flow fields. Electrochim. Acta **53**, 5334–5343 (2008)
7. Wang, X.D.; Zhang, X.X.; Liu, T.; Duan, Y.Y.; Yan, W.M.; Lee, D.J.: Channel geometry effect for proton exchange membrane fuel cell with serpentine flow field using a three-dimensional two-phase model. ASME J. Fuel Cell Sci. Technol. **7**, 051019 (2010)
8. Spernjak, D.; Prasad, A.K.; Advani, S.G.: In situ comparison of water content and dynamics in parallel, single serpentine, and interdigitated flow fields of polymer electrolyte membrane fuel cells. J. Power Sources **195**, 3553–3568 (2010)
9. Kahraman, Huseyin; Orhan, Mehmet F.: Flow field bipolar plates in a proton exchange membrane fuel cell: analysis & modeling. Energy Convers. Manag. **133**(1), 363–384 (2017)
10. Bunmark, N.; Limtrakul, S.; Fowler, M.W.; Vatanatham, T.; Gostick, J.: Assisted water management in a PEMFC with a modified flow field and its effect on performance. Int. J. Hydrogen Energy **35**, 6887–6896 (2010)
11. Kahraman, H.; Cevik, I.; Dündar, F.; Ficici, F.: The corrosion resistance behaviors of metallic bipolar plates for PEMFC coated with physical vapor deposition (PVD): an experimental study. Arab. J. Sci. Eng. **41**(5), 1961–1968 (2016)
12. Belchor, P.M.; Madalena, M.; Forte, C.; Carpenter, D.E.O.S.: Parallel serpentine-baffle flow field design for water management in a proton exchange membrane fuel cell. Int. J. Hydrogen Energy **37**, 11904–11911 (2012)
13. Chen, Pang-Chia: Robust integral voltage tracking control for PEM fuel cell systems under varying operating current. Arab. J. Sci. Eng. **39**(4), 3307–3322 (2014)

14. Akhtar, N.; Qureshi, A.; Scholta, J.; Hartnig, C.; Messerschmidt, M.; Lehnert, W.: Investigation of water droplet kinetics and optimization of channel geometry for PEM fuel cell cathodes. Int. J. Hydrogen Energy **34**, 3104–3111 (2009)
15. Liu, X.; Guo, H.; Ye, F.; Ma, C.: Flow dynamic characteristics in flow field of proton exchange membrane fuel cells. Int. J. Hydrogen Energy **33**, 1040–1051 (2008)
16. Suresh, P.V.; Jayanti, S.: Effect of air flow on liquid water transport through a hydrophobic gas diffusion layer of a polymer electrolyte membrane fuel cell. Int. J. Hydrogen Energy **35**, 6872–6886 (2010)
17. Chen, Y.S.; Peng, H.: Predicting current density distribution of proton exchange membrane fuel cells with different flow field designs. J. Power Sources **196**, 1992–2004 (2011)
18. Lobato, J.; Canizares, P.; Rodrigo, M.A.; Pinar, F.J.; Ubeda, D.: Study of flow channel geometry using current distribution measurement in a high temperature polymer electrolyte membrane fuel cell. J. Power Sources **196**, 4209–4217 (2011)
19. Peng, L.; Mai, J.; Hu, P.; Lai, X.; Lin, Z.: Optimum design of the slotted-interdigitated channels flow field for proton exchange membrane fuel cells with consideration of the gas diffusion layer intrusion. Renew. Energy **36**, 1413–1420 (2011)
20. Úbeda, D.; Cañizares, P.; Rodrigo, M.A.; Pinar, F.J.; Lobato, J.: Durability study of HTPEMFC through current distribution measurements and the application of a model. Int. J. Hydrogen Energy **39**, 21678–21687 (2014)
21. Arvay, A.; French, J.; Wanga, J.-C.; Peng, X.-H.; Kannan, A.M.: Nature inspired flow field designs for proton exchange membrane fuel cell. Int. J. Hydrogen Energy **38**, 3717–3726 (2013)
22. Wang, Chin-Tsan; Yuh-Chung, Hu; Zheng, Pei-Lun: Novel biometric flow slab design for improvement of PEMFC performance. Appl. Energy **87**, 1366–1375 (2010)
23. Ramos-Alvarado, B.; Hernandez-Guerrero, A.; Elizalde-Blancas, F.; Ellis, M.W.: Constructal flow distributor as a bipolar plate for proton exchange membrane fuel cells. Int. J. Hydrogen Energy **36**, 12965–12976 (2019)
24. Roshandel, R.; Arbabi, F.; Karimi, Moghaddam G.: Simulation of an innovative flow-field design based on a bio inspired pattern for PEM fuel cells. Renew. Energy **41**, 86–95 (2012)
25. Perng, Shiang-Wuu; Wub, Horng-Wen; Wang, Ren-Hung: Effect of modified flow field on non-isothermal transport characteristics and cell performance of a PEMFC. Energy Convers. Manag. **80**, 87–96 (2014)
26. Zeroual, M.; Ben Moussa, H.; Tamerabet, M.: Effect of gas flow velocity in the channels of consumption reactants in a fuel cell type (PEMFC). Energy Procedia **18**, 317–326 (2012)
27. Horng-Wen, Wu; Hui-Wen, Ku: The optimal parameters estimation for rectangular cylinders installed transversely in the flow channel of PEMFC from a three-dimensional PEMFC model and the Taguchi method. Appl. Energy **88**, 4879–4890 (2011)
28. Jang, Jer-Huan; Yan, Wei-Mon; Li, Hung-Yi; Chou, Yeh-Chi: Humidity of reactant fuel on the cell performance of PEM fuel cell with baffle-blocked flow field designs. J. Power Sources **159**, 468–477 (2006)
29. Liu, Hui-Chung; Yan, Wei-Mon; Soong, Chyi-Yeou; Chen, Falin: Effects of baffle-blocked flow channel on reactant transport and cell performance of a proton exchange membrane fuel cell. J. Power Sources **142**, 125–133 (2005)
30. Jang, Jiin-Yuh; Cheng, Chin-Hsiang; Huang, Yu-Xian: Optimal design of baffles locations with interdigitated flow channels of a centimeter-scale proton exchange membrane fuel cell. Int. J. Heat Mass Transf. **53**, 732–743 (2010)
31. Pinchuk, O.A.; Dundar, F.; Ata, A.; Wynne, K.J.: Improved thermal stability, properties, and electrocatalytic activity of sol-gel silica modified carbon supported Pt catalysts. Int. J. Hydrogen Energy **37**, 2111–2120 (2012)
32. Dundar, F.; Uzunoglu, A.; Ata, A.; Wynne, K.J.: Durability of carbon–silica supported catalysts for proton exchange membrane fuel cells. J. Power Sources **202**, 184–189 (2012)
33. Li, X.; Sabir, I.: Review of bipolar plates in PEM fuel cells: flow-field designs. Int. J. Hydrogen Energy **30**, 359–371 (2005)
34. Sherman, T.F.: On connecting large vessels to small: the meaning of Murray's law. J. Gen. Physiol. **78**, 431–453 (1981)
35. Barber, R.W.; Emerson, D.R.: Optimal design of microfluidic networks using biologically inspired principles. Microfluid. Nanofluid. **4**, 179–191 (2008)
36. Emerson, D.R.; Cieslicki, K.; Gu, X.J.; Barber, R.W.: Biomimetic design of microfluidic manifolds based on a generalized Murray's law. Lab Chip **6**, 447–454 (2006)
37. Barber, R.W.; Emerson, D.R.: Biomimetic design of artificial micro-vasculatures for tissue engineering. ATLA **38**(Suppl. 1), 67–79 (2010)
38. Nannan, G.; Ming, C.L.; Koylu, U.O.: Bio-inspired flow field designs for polymer electrolyte membrane fuel cells. Int. J. Hydrogen Energy **39**(36), 21185–21195 (2014)
39. Lee, J.; Gundu, M.H.; Lee, N.; Lim, K.; Ju, H.: Innovative cathode flow-field design for passive air-cooled polymer electrolyte membrane (PEM) fuel cell stacks. Int. J. Hydrogen Energy, corrected proof. Available online 13 August 2019 **(in press)**
40. Debe, M.K.: Electrocatalyst approaches and challenges for automotive fuel cells. Nature **486**, 43–51 (2012)
41. Ortiz, C.; Joseph, D.D.; Beavers, G.S.: Acceleration of a liquid drop suddenly exposed to a high speed airstream. Int. J. Multiphase Flow **30**, 217–224 (2004)
42. Joseph, D.D.; Belanger, J.; Beavers, G.S.: Breakup of a liquid drop suddenly exposed to a high speed airsteam. Int. J. Multiphase Flow **25**, 1263–1303 (1999)
43. Zhang, S.; Yuan, X.Z.; Hin, J.N.C.; Wang, H.; Friedrich, K.A.; Schulze, M.: A review of platinum-based catalyst layer degradation in proton exchange membrane fuel cells. J. Power Sources **194**, 588–600 (2009)
44. Dhahad, Hayder A.; Alawee, Wissam H.; Hassan, Ali K.: Experimental study of the effect of flow field design to PEM fuel cells performance. Renew. Energy Focus **30**, 71–77 (2019)